

An Investigation of Global Albedo Values

Mark K. Mulrooney

ESCG/MEI, Houston, TX (mark.mulrooney-1@nasa.gov)

Mark J. Matney

NASA Johnson Space Center, Houston, TX (mark.matney-1@nasa.gov)

Matthew D. Hejduk

SRA International, Colorado Springs, CO (mdhejduk@earthlink.net)

Edwin S. Barker

NASA Johnson Space Center, Houston, TX (edwin.s.barker@nasa.gov)

ABSTRACT

Mulrooney and Matney [1] developed a technique for estimating the intrinsic size distribution of orbital fragmentation debris and among the conclusions of their study was the recommendation of a global albedo value of 0.13 for these debris objects. In 2008 this value was revised upward to 0.175 [2] after revisions were made to the basis set of supplied brightness data (NASA-Liquid Mirror Telescope photometry data [3-5]). These revisions primarily involved uniform application of Lambertian phase function correction as opposed to the specular/Lambertian mixture in the original dataset. While these two studies demonstrated the soundness of their approach, uncertainties in the optical and radar data used for the calculations led the studies to produce only a provisional, rather than definitive, global albedo value for fragmentation debris. Calculations using alternate photometric and RCS (Radar Cross Section) data is required to support the use of their albedo in a truly global context. As a first step in this vetting process we perform an albedo consistency check by utilizing RCS values from an alternate source - the United States Air Force Space Command Studies and Analysis Division (AFSPC/A9A) high-precision RCS catalogue. As with prior work, these values will be passed through NASA's Size Estimation Model which primarily provides a diameter correction (downward) for objects in the Rayleigh scattering regime. Analysis using other photometric sources, such as the GEODSS visual magnitude data repository, will be performed in future.

In addition to fragmentation debris, there is utility in exploring the albedo distribution of non-fragmentation objects – including intact rocket bodies, payloads, and mission related objects. Queries about space object size are often tendered against object types other than merely fragmentation debris; frequently, full-catalogue size profiling is desired, which includes payloads and rocket bodies. When published size information about these objects is available, these actual measurements can be used for such profiling; but since they are often unavailable, it would be helpful to have an expansion of the Mulrooney and Matney technique available for this class of objects. As a first step in this process, we will determine the character of the albedo distribution for non-fragmentation targets based on LMT photometry and available data from the A9 high-precision RCS catalogue. Since the size distribution for this object class does not follow a simple power-law, a suitable subset will be extracted whose behavior is approximated by a weak power-law and a bias corrected albedo will be derived.

1. INTRODUCTION

Orbital object data acquired via radar and optical telescopes plays a crucial role in accurately defining the space environment. Extremely short arc ($< 0.5\text{deg}$) optical observations, such as those obtained by NASA's 3.0 meter Liquid Mirror Telescope (LMT) [3-5] yield an angular velocity which, with an Assumed Circular Orbit (ACO), gives a range. This range, combined with the apparent brightness and a phase function assumption, yields debris size if an albedo is assumed. Conversely if object size is divined from an available RCS, then albedo is derived.

However, shape and albedo variations make any given size or albedo estimate subject to large random errors. As has been shown with radar/optical debris measurements, that does not preclude the ability to optically estimate the size of an individual object via an ensemble of measurements, or the size or albedo distribution of a large number of objects statistically[6-9].

After the systematic errors resulting from ACO and phase function assumptions have been estimated, there remains a Bond albedo distribution that relates object size to absolute (range/phase corrected) magnitude. Measurements acquired by the LMT [7] of a large subset of tracked debris objects with sizes estimated from their RCS indicate that the random variations in the albedo follow a Log-Normal distribution (hereafter L-N). This thesis appears to hold for the broadest classes of objects studied thus far – debris resulting from fragmentations and intact (non-fragmentation) objects. Perhaps counter-intuitive, the L-N form of the distribution is the same whether the shapes and other properties are the result of human manufacture or of random (e.g explosive) processes. In addition, these distributions are independent of object size over the ranges thus far assessed (a few centimeters to several meters). With this information in hand, it now becomes possible, via optical measurements, to accurately estimate the actual size distribution of debris objects.

2. PHOTOMETRY AND SIZE ESTIMATION

The photometric reduction of telescopic optical orbital object data normally involves the comparison of target brightness with that of known background stars. Since astronomical objects used as fiduciary references typically have their brightness categorized using color filter photometry, observations are normally conducted with broad-band colored filters. Using this calibration basis, an observed or apparent color-dependent magnitude (M_{app}) is ascribed to the object of interest. For debris, M_{app} is usually derived for the visual band (V; typically 550 nm center, 125 nm width) or the red band (R; typically 650 nm center, 150 nm width).

The size of the debris object is estimated by computing the characteristic length (L_C), which is typically the diameter D of an equivalent Lambertian sphere having apparent magnitude, M_{app} , from the equation

$$D = 10^{(M_{Sun} - M_{app}) / 5} \frac{R}{\sqrt{A}} \sqrt{\frac{6\pi}{\sin(PA) + (\pi - PA) \cos(PA)}} \quad \text{Eq. 1}$$

where PA is the solar phase angle, A is the Bond albedo (ratio of incident to scattered power over all PA), R is the range, and M_{Sun} is the apparent magnitude of the Sun (e.g., -26.75 in the Johnson V band centered at 550 nm.). If an albedo for the object is assumed, the photometric brightness of the object can be converted into an optical cross section. Conversely, if characteristic length is determined via RCS measurements (or actual launch data for payloads and rocket bodies), then the Bond albedo is similarly determined via:

$$A = 10^{(M_{Sun} - M_{app}) / 2.5} \frac{R^2}{D^2} \frac{6\pi}{\sin(PA) + (\pi - PA) \cos(PA)} \quad \text{Eq. 2}$$

Sometimes it is useful to normalize range (R in km) to a standard 1000 km, in which case an absolute magnitude (M_{abs}) is also reported:

$$M_{abs} = M_{app} - 5 \log \left(\frac{R}{1000} \right) \quad \text{Eq. 3}$$

3. MATHEMATICAL FRAMEWORK OF THE TRANSFORMATIONAL ALBEDO

For albedo distributions that are L-N and object size distributions that obey a P-L, there exists a mathematically elegant and straightforward technique for ascertaining the intrinsic size distribution via optical measurements. The accuracy of the method is predicated only on the accuracy of the underlying observations. An alternate methodology

can be applied to non P-L distributions (non-fragmentation objects) but its development is beyond the scope of this paper.

The observed distribution of optical brightness is the product integral of the size distribution of the parent population with the albedo probability distribution. If the former and latter are P-L and N-L respectively, it is a straightforward matter to transform a given distribution of optical brightness back to a size distribution by the appropriate choice of a single albedo value. This is true because the integration of a P-L with a L-N distribution (Fredholm Integral of the First Kind) yields a Gaussian-blurred P-L distribution with identical P-L exponent. Application of a single albedo to this distribution recovers a simple P-L [in size] which is linearly offset from the original distribution by a constant whose value depends on the choice of the albedo. Significantly, there exists a unique Bond albedo which, when applied to an observed brightness distribution, yields zero offset and therefore recovers the original size distribution. For physically realistic P-Ls of negative slope, the proper choice of albedo recovers the parent size distribution by compensating for the observational bias caused by the large number of small objects that appear anomalously “large” (bright) - and thereby skew the small population upward by rising above the detection threshold - and the lower number of large objects that appear anomalously “small” (dim).

Via this methodology, an observed distribution of object magnitudes (and by corollary, range and phase corrected intrinsic brightness) can ultimately be transformed to a distribution of object sizes free of any systematic bias. Although there are certainly errors introduced by the application of ACO range estimates, a phase function, and photometric measurements themselves, the errors are either well characterized (e.g., range bias due to non-zero eccentricity) or are randomly distributed and generally size independent (e.g., specular reflections from debris). This enables judicious choice of an albedo to transform observed brightness distributions back to the intrinsic size distribution of the parent population. Given an adequate initial photometric and RCS sample, it should be possible to derive a global albedo applicable to any ensemble of optical observations.

The fundamental principle underlying the process is that the observed number distribution of object brightness $N(M_{abs})dM_{abs}$ is the product integral (Equation 4) of a parent size P-L($N(D_0)$) with a L-N albedo spread $P(A|A_0)$ – yielding a Gaussian-blurred size distribution. This is the hidden structure underlying the familiar number versus magnitude plots or, analogously, number versus size plots and it is the key to extracting the intrinsic parent size distribution.

$$N(M_{abs})dM_{abs} = \int_D P(M_{abs} | D_0) \cdot N(D_0) \cdot dD_0 \quad \text{Eq. 4}$$

where $P(M_{abs} | D_0) \propto P(A | A_0) \cdot \frac{D_0^2}{4} A$ is the probability (P) of measuring apparent magnitude M_{app} given actual object diameter D_0 , median geometric albedo A_0 , and actual albedo A (an element of the L-N distribution in A).

Applying a constant albedo value to a brightness distribution yields a diameter distribution. The accuracy of that distribution (i.e., the extent to which it is systematically biased) depends on the choice of albedo – which itself depends upon the P-L slope β . Fig. 1 illustrates the distribution of perceived object size (D) relative to the parent (or true) object size (D_0) resulting from the transformation of a brightness distribution to a size distribution. This is simply a re-casting of a brightness distribution into the size domain. The Gaussian blur is now in size rather than magnitude.

Naturally, the underlying structure – in the form of a Gaussian blur - in magnitude or size is not a directly observable quality. Telescopic observations effectively integrate slices through constant apparent magnitude – or - after albedo transformation – through constant derived diameter. That integral is itself a P-L and that is what is directly measured. This observed P-L will have zero systematic offset, and thereby match the parent, if the transformational albedo is chosen properly. Furthermore, because the offset is independent of diameter, the bias introduced by poor albedo choice is constant over all size ranges.

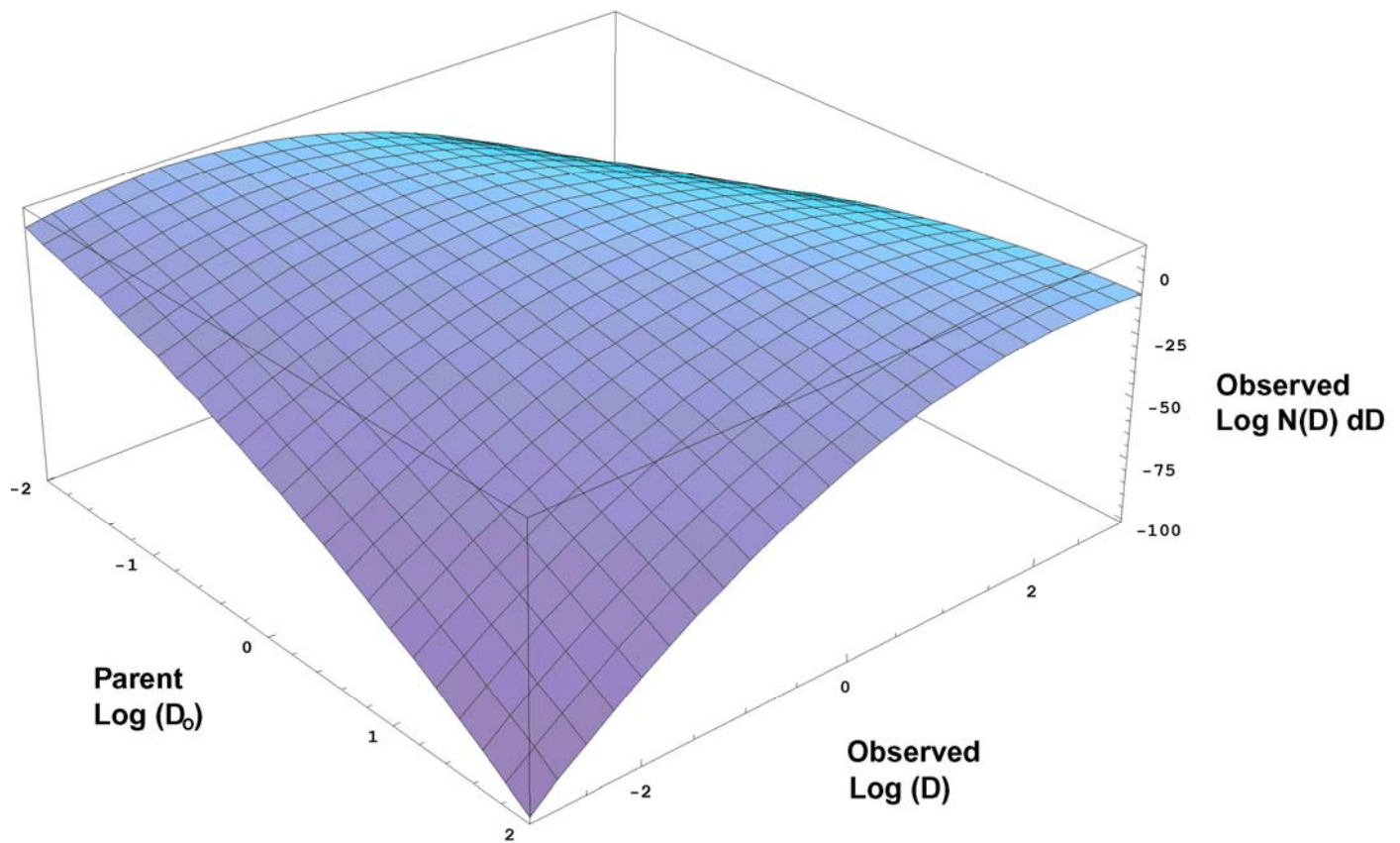


Fig. 1. Probability Distribution of Observed Diameters. This figure demonstrates the spread of apparent object size (D) relative to the actual object size (D_0) when the albedo distribution is considered - for each parent diameter there is a distribution of observed diameters. The full convolution of the log-normal and power-law functions (i.e., the number-size distribution we actually observe) is the integrated area under a slice at constant diameter D . If the reference albedo is not chosen carefully, the derived distribution of object size will be disproportionately influenced by objects whose true size (D_0) is smaller (or larger) than the diameter of interest. For moderately negative power laws this results in a positive or negative bias in the calculated number distribution. By judicious choice of a reference albedo the parent distribution can be recovered. This figure was generated with the 0.175 bias-free albedo.

4. GENERATION OF TRANSFORMATIONAL ALBEDOS FROM OPTICAL/RADAR DATA SETS

Mulrooney and Matney[1] derived a global transformational albedo of 0.13 based on an extended fragmentation-only photometric dataset consisting of 258 NASA-LMT photometric observations acquired from 1998-2001. For prior studies, the data had been first range and phase corrected with a mixed Lambertian and Specular phase function, after which a 0.1 albedo was applied to yield an observed size distribution [6,7]. For the new study, the albedo was backed out and SEM corrected RCS values from various sources were applied to yield an individual albedo for each object. The distribution was hence assessed and shown to be L-N (Figs. 2 and 3). Its median and standard deviation were then coupled with an assumed P-L size distribution using the generally accepted $\beta = -1.6$ exponent [10,11] to yield the reported bias-free 0.13 albedo. Mulrooney, et.al[2] re-processed the prior supplied data and applied a uniform Lambertian phase function to yield an updated value of 0.175 (Fig 4). This value fully bias corrects an observed brightness distribution and recovers the underlying $\beta = -1.6$ P-L size distribution. It is interesting to note that the size distribution for the employed dataset, based on the SEM corrected RCS values available at the time, follows a P-L with $\beta = -1.81$ (Fig. 5). The transformational bias-free albedo value thus derived is 0.185 – implying the bias-free is insensitive to small changes in P-L exponent.

As part of the current study, the RCS values used prior were replaced with values from the AFSPC/A9A high-precision RCS catalogue. SEM corrected values from the Eglin 442 MHz Radar were used exclusively since they are derived using median returns from both principal and orthogonal polarizations. Using median values eliminates the significant upward size bias resulting from taking arithmetic means of typically log-normally distributed size measurements in meters-squared space. As expected, the P-L nature of the distribution did not change, but the median albedo value changed significantly to $\bar{A} = 0.145$ ($\text{Log } \bar{A} = -8.38$) as did the average ($\langle A \rangle = 0.209$), but the log-width is similar ($\text{Log } \sigma = 5.5$). The resulting bias corrected albedo for distributions with the -1.6 P-L exponent is 0.275. Clearly the accuracy of the transformational albedo is extremely sensitive to the quality of the RCS values employed to generate the initial L-N albedo distribution. The 0.275 value represents a significant increase beyond the canonical norm of 0.1, necessitating further validation of the Eglin SEM derived sizes and LMT photometric measurements.

To investigate the albedo properties of non-fragmentation objects, they (249 total) were culled from the LMT photometric database and analyzed using an approach similar to that of the fragmentation component. The albedo distribution is very well fit by a P-L (Fig 6) – and the median and average albedo are lower than that of the fragmentation distribution at $\bar{A} = 0.095$ ($\text{Log } \bar{A} = -10.2$) and $\langle A \rangle = 0.142$ respectively. The log-width is actually narrower ($\text{Log } \sigma = 4.6$) – imply less scatter. One would not expect a priori that an entirely different class of objects – they are larger and structurally intact – would exhibit a P-L albedo distribution. It is also surprising that the albedo is lower. Datasets from other sources will be required to validate this result. For clarity, results are tabulated in Fig 7.

The P-L distribution of non-fragmentation albedos is a useful, albeit unexpected, result. While there is utility in the average 0.142 albedo indicated by this dataset, bias correction is more difficult because the parent size distribution is functionally more complex than a P-L (Fig 8a). For investigative purposes, it is useful to extract that portion of the distribution that exhibits P-L properties. Conveniently the LMT dataset supports a P-L with an exponent $\beta = -0.83$ from -0.6 to .3 in Log D (0.3 to 2.0 m diameter) (Fig. 8b). The bias adjusted albedo derived thereof is 0.12.

5. CONCLUSION

Rather than fortify confidence in a specific global albedo value, the results obtained in this study clearly indicate that more research is required. Photometric datasets from alternate sensors and perhaps RCS values from other radars will be required to identify the systematic biases that may be present in any given measurement set. Additionally, data on launch size and geometry will need to be employed in the analysis as an independent size reference. The behavior of the ensemble of non-fragmentary objects reviewed here while counter-intuitive may indeed be supported by additional data. The discrepancy between albedos derived for fragments using different radar sources, demands a more thorough evaluation of the available data. The mathematical formalism used to remove observational bias for populations conforming to a P-L is well established, so it remains to amass sufficient observations to generate a statistically accurate albedo assessment and thereby make the claim of global applicability.

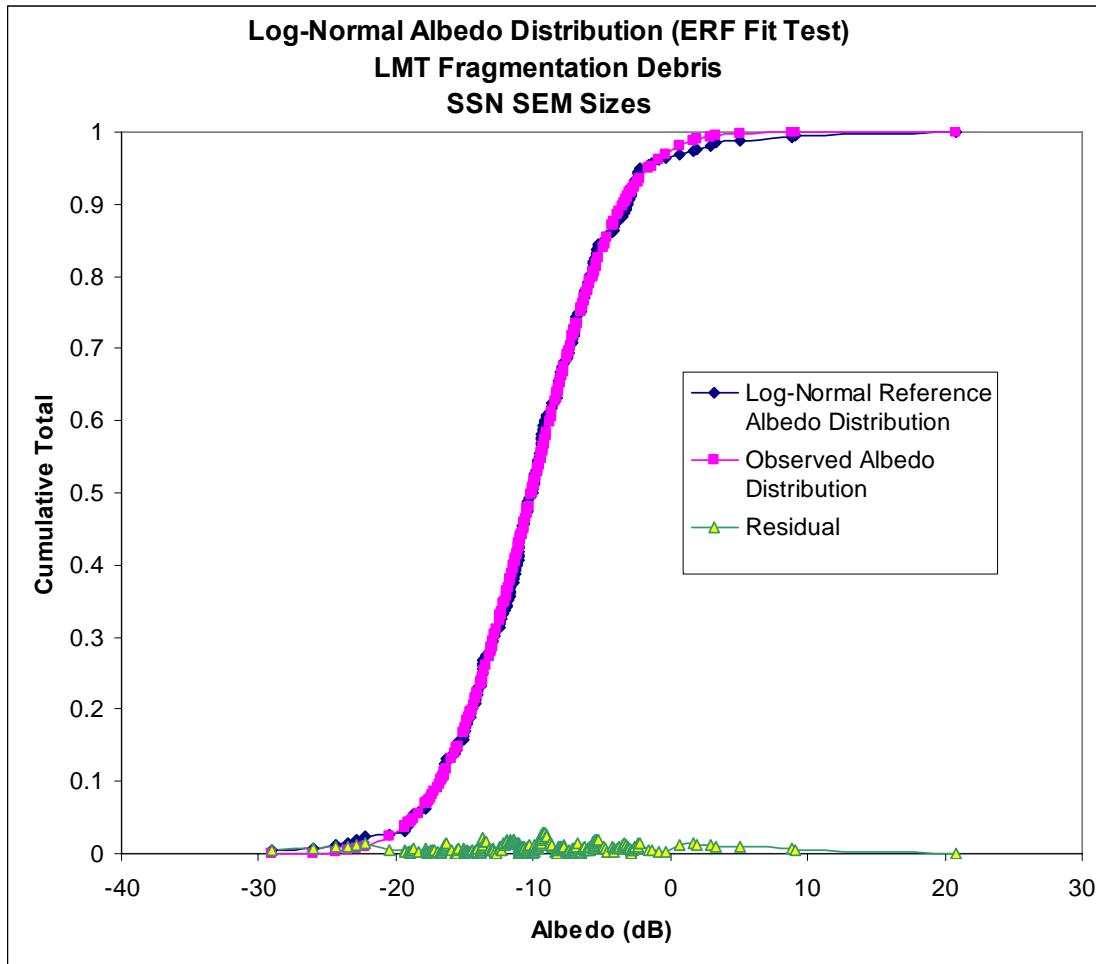


Fig. 2. Error Function (ERF) fit demonstrating the L-N structure of the albedo distribution derived from fragmentation debris observed by the NASA-LMT. The median albedo \bar{A} is 0.098 ($\text{Log } \bar{A} = -10.07$), log-width ($\text{Log } \sigma$) is -0.52, and the average value $\langle A \rangle = 0.152$.

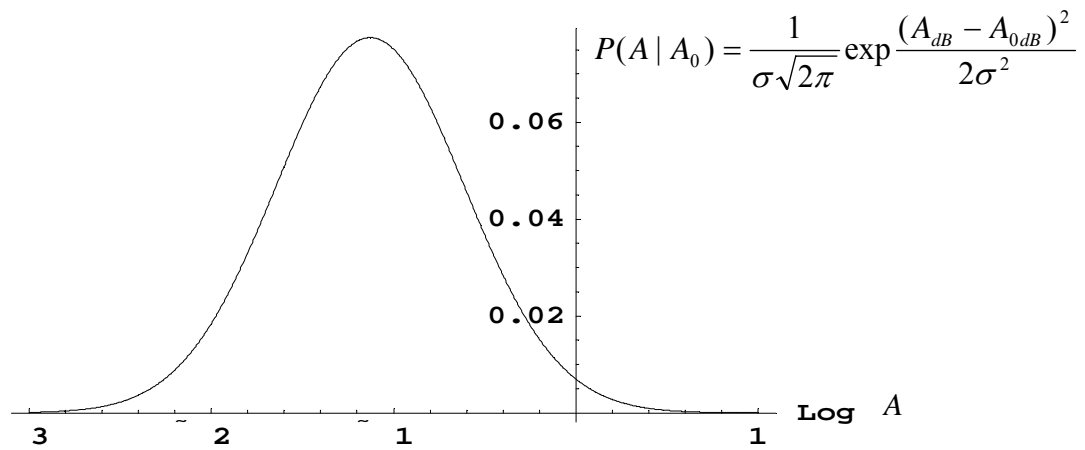


Fig. 3. The albedo distribution (i.e., the probability of finding A given A_0) of fragmentation debris. The median albedo \bar{A} is 0.098 ($\text{Log } \bar{A} = -10.07$), log-width ($\text{Log } \sigma$) 5.2, and the average value $\langle A \rangle = 0.152$.

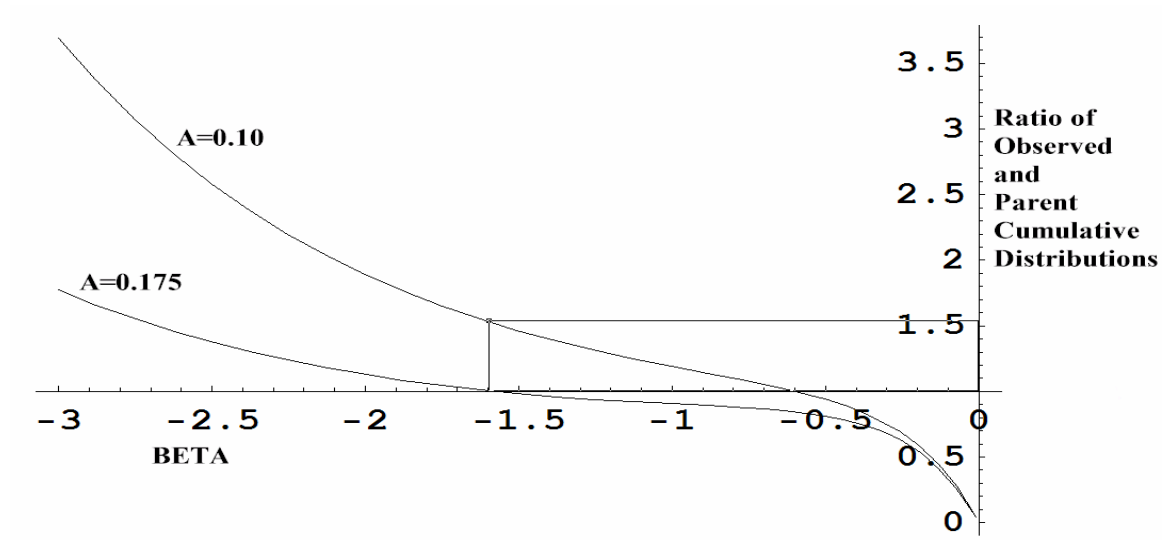


Fig. 4. Ratio of observed cumulative power-law size distribution to the parent power-law distribution. Selection of a 0.10 albedo yields a ratio of 1.54 for a parent power-law with a $\beta = -1.6$ slope - thus the population is overestimated by 54% - this is "small object" bias. Selection of a 0.175 albedo conversely yields a bias-free ratio (unity). The parent number distribution is recovered with judicious choice of albedo.

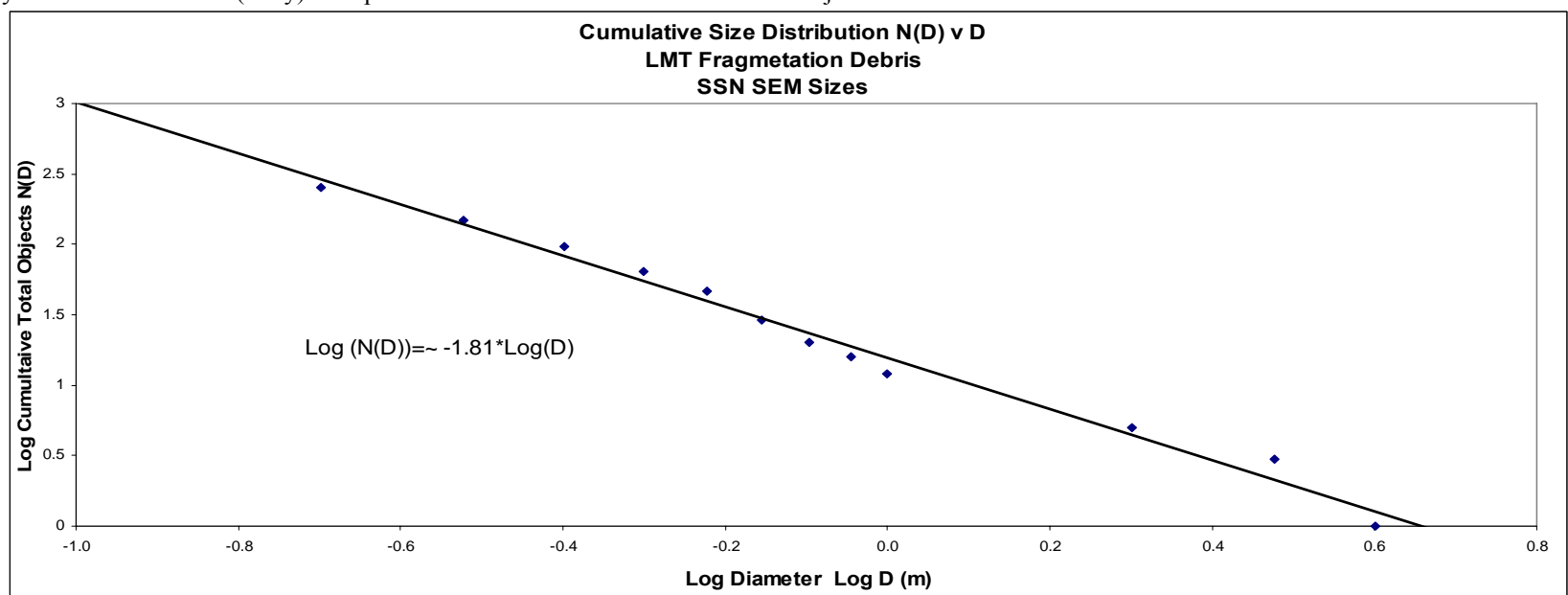


Fig. 5. Cumulative Size Distribution for the 258 member set of fragmentation debris as indicated by the SEM sizes from multiple RCS sources. The distribution is well fit by a P-L with $\beta = -1.6$.

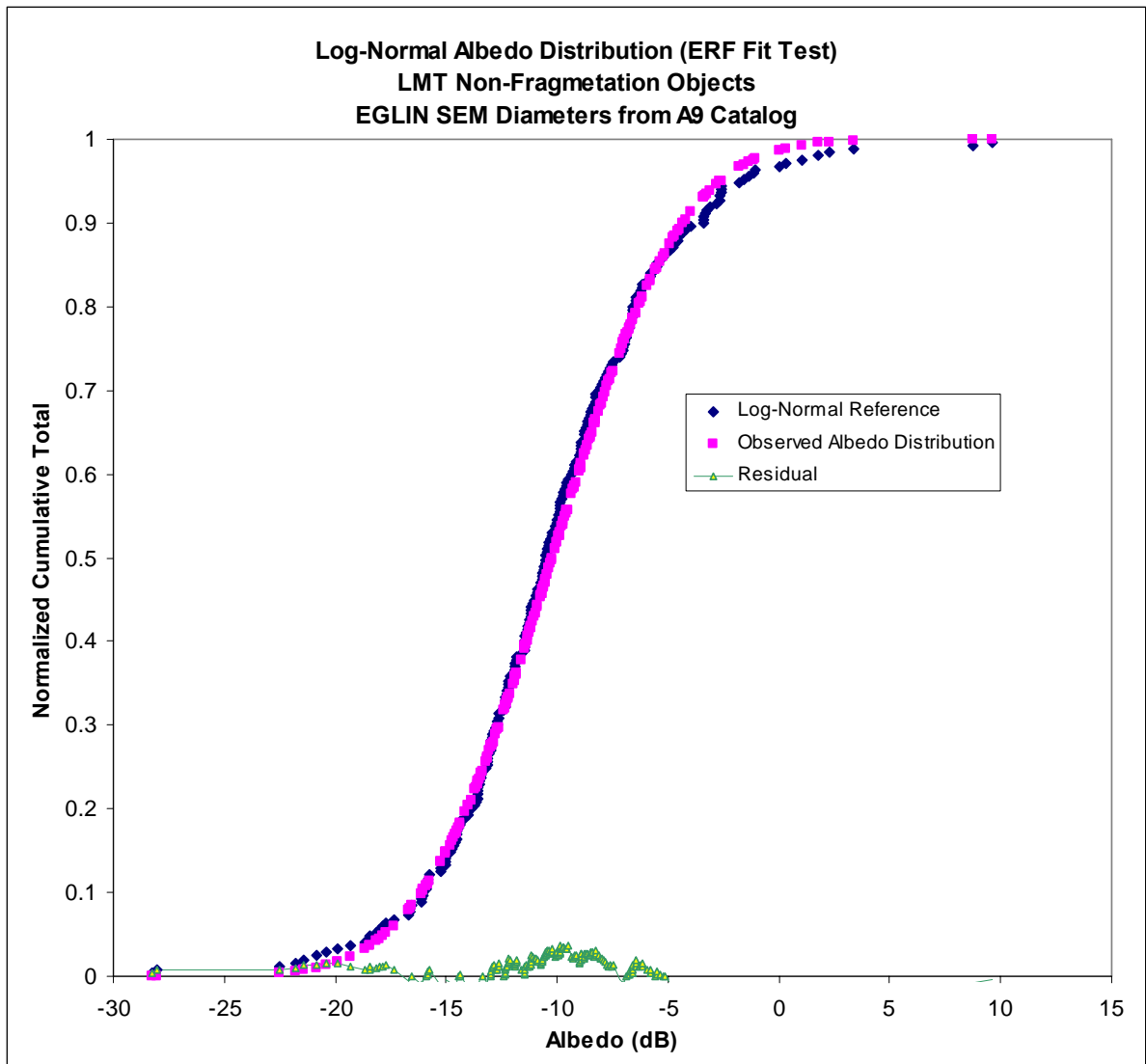


Fig. 6. Error Function (ERF) fit demonstrating the L-N structure of the albedo distribution derived from non-fragmentation debris observed by the NASA-LMT. The median albedo $\bar{A} = 0.095$ ($\text{Log } \bar{A} = -10.2$), the average $\langle A \rangle = 0.142$, and log-width ($\text{Log } \sigma$) is 4.6. This result is somewhat counterintuitive, since the objects are formed from regular rather than random processes.

OBJECT CLASS	SENSOR		PHASE FN	ALBEDO				BIAS CORRECT A @ β
	Optical	Radar		Log \bar{A} (dB)	\bar{A}	Log σ	$\langle A \rangle$	
Fragmentation	LMT	ALL	Mixed Spec/Lambertian	-11.12	0.076	5.15	0.123	0.13 @ -1.6
“	LMT	ALL	Lambertian	-10.07	0.098	5.2	0.152	0.175 @ -1.6 0.185 @ -1.81
“	LMT	Eglin	Lambertian	-8.38	0.145	5.5	0.209	0.275 @ -1.6
Non-Fragmentation	LMT	Eglin	Lambertian	-10.2	0.095	4.6	0.142	0.12 @ -0.83 (0.3 to 2.0 m)

Fig 7. Tabulation of final results indicating dependence of transformational albedo on object class, phase function, and RCS source.

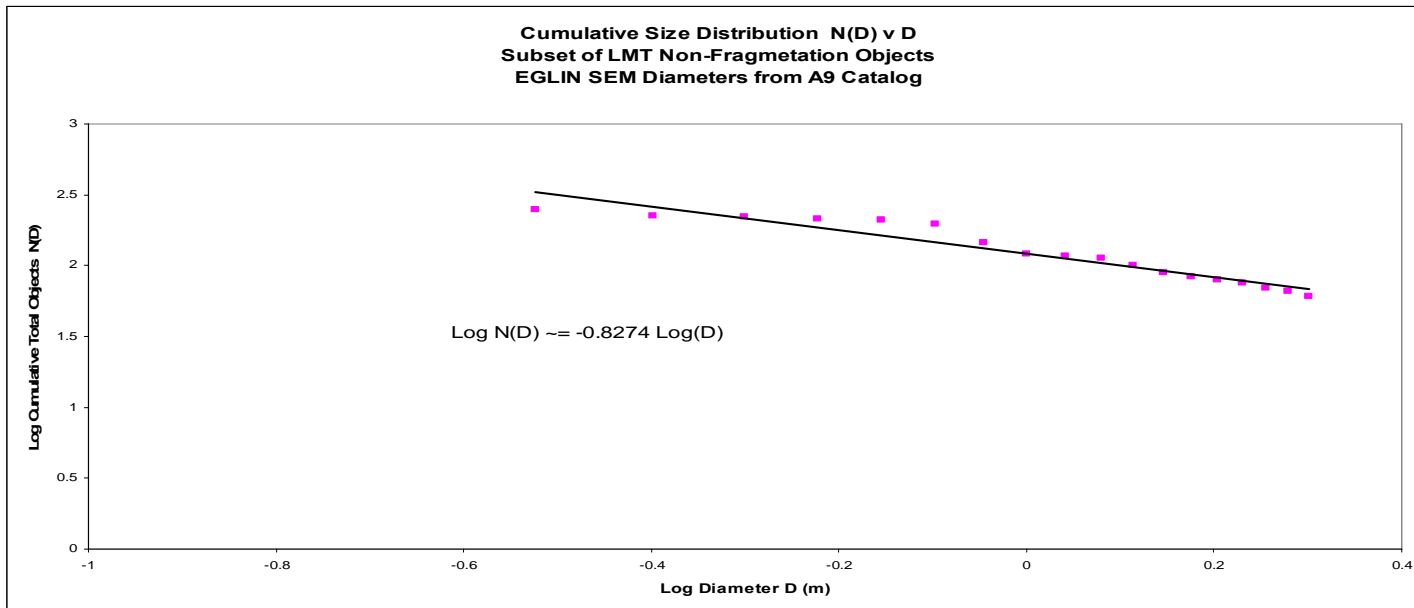
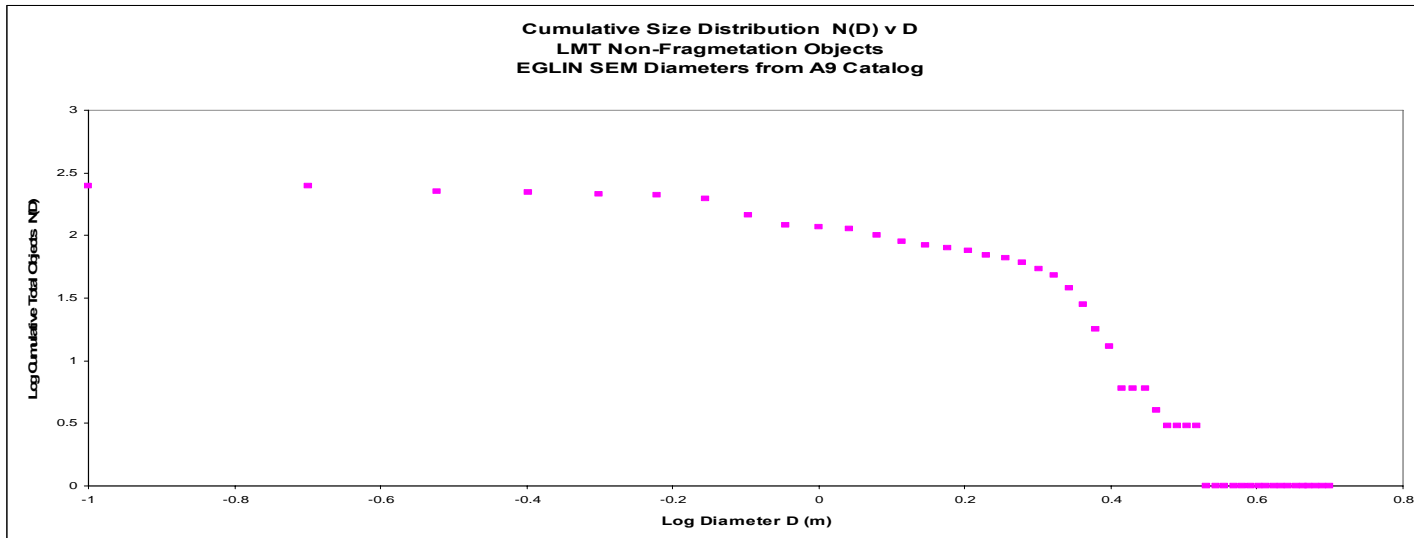


Fig. 8a and 8b. Cumulative Size Distribution (top) for the 249 member set of non-fragmentation debris as indicated by the Eglin SEM sizes from the AFSPC/A9A (A9) precision RCS catalog. The full distribution cannot be bias corrected using the formalism described here, but a broad subset (bottom) is well fit by a P-L with exponent $\beta = -0.83$ on the range -0.6 to $.3$ in $\text{Log } D$ (0.3 to 2.0 m diameter). The bias adjusted albedo derived thereof is 0.12.

REFERENCES

1. M. Mulrooney and M. Matney, "Derivation and Application of a Global Albedo Yielding an Optical Brightness to Physical Size Transformation Free of Systematic Errors." Proceedings of 2007 AMOS Technical Conference, Kihei, HI, pp. 719-728, 2007.
2. M. Mulrooney, M. Matney, and E. Barker, "A New Bond Albedo for Performing Orbital Debris Brightness to Size Transformations." 2008 International Astronautical Congress, Glasgow, Scotland, October 2008 (in preparation).
3. A. E. Potter and M. K. Mulrooney. "Liquid Metal Mirror for Optical Measurements of Orbital Debris." *Advances in Space Research*, Vol. 19, pp. 213-219, 1997.
4. E. S. Barker, K. S. Jarvis, K. J. Abercromby, T. L. Parr-Thumm, J. L. Africano, and E. G. Stansbery "The LEO Environment as Determined by the LMT between 1998 and 2002." Proceedings of the 2005 AMOS Technical Conference, Wailea, Maui, HI, pp. 206-215, 2005.
5. K. S. Jarvis, T. L. Thumm, E. S. Barker, J. L. Africano, M. J. Matney, E. G. Stansbery, K. Abercromby, and M. K. Mulrooney. "Liquid Mirror Telescope (LMT) Observations of the Low Earth Orbit Orbital Debris Environment March 1999 – September 2000." *JSC-29713*, Houston, TX, 2006.
6. K. Henize, M.K. Mulrooney, C. O'Neill, and P. Anz-Meador. "Optical Properties of Orbital Debris", 1993, AIAA-93-0162.
7. K. Henize, J. Stanley, C. O'Neill, and B. Nowakowski. "Detection of Orbital Debris with GEODSS Telescopes." SPIE, Orlando, FL, pp. 76-84, 1993.
8. G. Bohannon, Comparisons of Orbital Debris Size Estimation Methods Based on Radar Data, Report # 920123-BE-2048, XonTech, Inc., 1992.
9. D. K. Barton, D. Brillinger, P. McDaniel, K. H. Pollock, A. H. El-Shaarawi, and M. T. Tuley. "Final Report of the Haystack Orbital Debris Data Review Panel." NASA TM-4809, Houston, TX, 1998.
10. N.L. Johnson, P.H. Krisko, J.-C. Liou, and P.D. Anz-Meador. "NASA's New Breakup Model OF Evolve 4.0." *Advanced Space Research*, Vol 28, No. 9, pp. 1377-1384, 2001.
11. J. Liou, M. Matney, P. Anz-Meador, D. Kessler, M. Jansen, and J. Theall. "The New NASA Orbital Debris Engineering Model ORDEM2000." NASA/TP 2002-210780, Houston, TX, 2002.